Current Biology, Vol. 14, 1694–1702, October 5, 2004, ©2004 Elsevier Ltd. All rights reserved. DOI 10.1016/j.cub.2004.09.048

Drosophila T Box Proteins Break the Symmetry of Hedgehog-Dependent Activation of *wingless*

Marita Buescher,[1,4,*] Pia C. Svendsen,[2,4] Murni Tio,[1] Cindy Miskolczi-McCallum,[2] Guy Tear,[1] William J. Brook,[2] and William Chia[1,3]
[1]Medical Research Council Centre
for Developmental Neurobiology
King's College London
4th Floor New Hunts House
Guy's Hospital Campus
London SE1 1UL
United Kingdom
[2]Genes and Development Research Group and
Department of Biochemistry and Molecular Biology
University of Calgary
3330 Hospital Drive NW
Calgary, Alberta T2N 4N1
Canada
[3]Temasek Lifesciences Laboratory
1 Research Link
National University of Singapore Campus
Singapore
Singapore 117604

Summary

Background: Segmentation of the *Drosophila* embryo is a classic paradigm for pattern formation during development. The Wnt-1 homolog Wingless (Wg) is a key player in the establishment of a segmentally reiterated pattern of cell type specification. The intrasegmental polarity of this pattern depends on the precise positioning of the Wg signaling source anterior to the Engrailed (En)/Hedgehog (Hh) domain. Proper polarity of epidermal segments requires an asymmetric response to the bidirectional Hh signal: *wg* is activated in cells anterior to the Hh signaling source and is restricted from cells posterior to this signaling source.
Results: Here we report that Midline (Mid) and H15, two highly related T box proteins representing the orthologs of zebrafish *hrT* and mouse Tbx20, are novel negative regulators of *wg* transcription and act to break the symmetry of Hh signaling. Loss of *mid* and *H15* results in the symmetric outcome of Hh signaling: the establishment of *wg* domains anterior and posterior to the signaling source predominantly, but not exclusively, in odd-numbered segments. Accordingly, loss of *mid* and *H15* produces defects that mimic a *wg* gain-of-function phenotype. Misexpression of *mid* represses *wg* and produces a weak/moderate *wg* loss-of-function phenocopy. Furthermore, we show that loss of *mid* and *H15* results in an anterior expansion of the expression of *serrate (ser)* in every segment, representing a second instance of target gene repression downstream of Hh signaling in the establishment of segment polarity.
Conclusions: The data we present here indicate that *mid* and *H15* are important components in pattern formation in the ventral epidermis. In odd-numbered abdominal segments, Mid/H15 activity plays an important role in restricting the expression of Wg to a single domain.

*Correspondence: marita.buescher@kcl.ac.uk
[4]These authors contributed equally to the work.

Background

The larval cuticle of *Drosophila melanogaster* is a model system for generating patterns from fields of cells. The ventral cuticle exhibits a segmentally reiterated array of six rows of unique denticles separated by areas of naked cuticle. These external structures reflect the cellular diversity within the underlying epidermis, and defective cuticle patterns are indicative of incorrectly specified cell fates [1]. The secreted products of two segment polarity genes, *wg* and *hh*, are the key players that initiate progressive patterning events that ultimately result in epidermal differentiation at the single-cell level [2–9]. Thus, patterning requires the tight regulation of the spatial limits of Wg and Hh expression. In early embryogenesis, pair-rule gene activity initiates the expression of Wg and Hh in adjacent stripes, with Wg just anterior to the Hh-expressing cells (the spatial arrangement of these expression domains is shown in Figure 7G). After stage 9, reciprocal signaling between Wg- and Hh-expressing cells stabilizes their expression domains. Acting anisotropically, Hh signaling activates Wg anterior, but not posterior, to the Hh stripe. Finally, Wg expression becomes independent of Hh and is maintained through an autoregulatory feedback loop. Previous studies have led to the conclusion that Hh signaling is bidirectional because it maintains *patched* (*ptc*)-gene expression in narrow stripes anterior and posterior to the En/Hh stripe [10, 11]. The *ptc* gene product is a repressor of Wg expression, and maintenance of Wg expression at stage 9 requires the Hh-mediated derepression. However, despite the symmetry of Hh signaling, the outcome with respect to Wg expression is asymmetric and results in a single Wg stripe anterior to the En/Hh stripe. To rationalize the differential response of Wg to the Hh signal, Ingham et al. have put forward a model that subdivides each parasegment into two domains: the posterior half of the parasegment represents the *wg*-competent domain, and the anterior half is the *en*-competent domain [12]. The *wg*-competent domain encompasses those cells that express Wg in a *ptc* mutant background. Later studies showed that *wg* competence requires the activity of the pair-rule/segment polarity genes *sloppy-paired 1, 2* (*slp1, 2*), which are expressed in broad stripes anterior to the En/Hh stripe (see model Figure 7G for the location of the *slp* expression domain) [13]. It has been suggested that Slp permits the activation of Wg anterior to the En/Hh stripe by antagonizing one (or several) putative repressor(s) of Wg. Here we report that Mid and H15 act to repress the Hh-dependent activation of Wg in the *en*-competent domain predominantly in odd-numbered segments. Furthermore, our results suggest that the Slp-mediated repression of Mid/H15 anterior to the En/Hh stripe is an important component of *wg* competence.

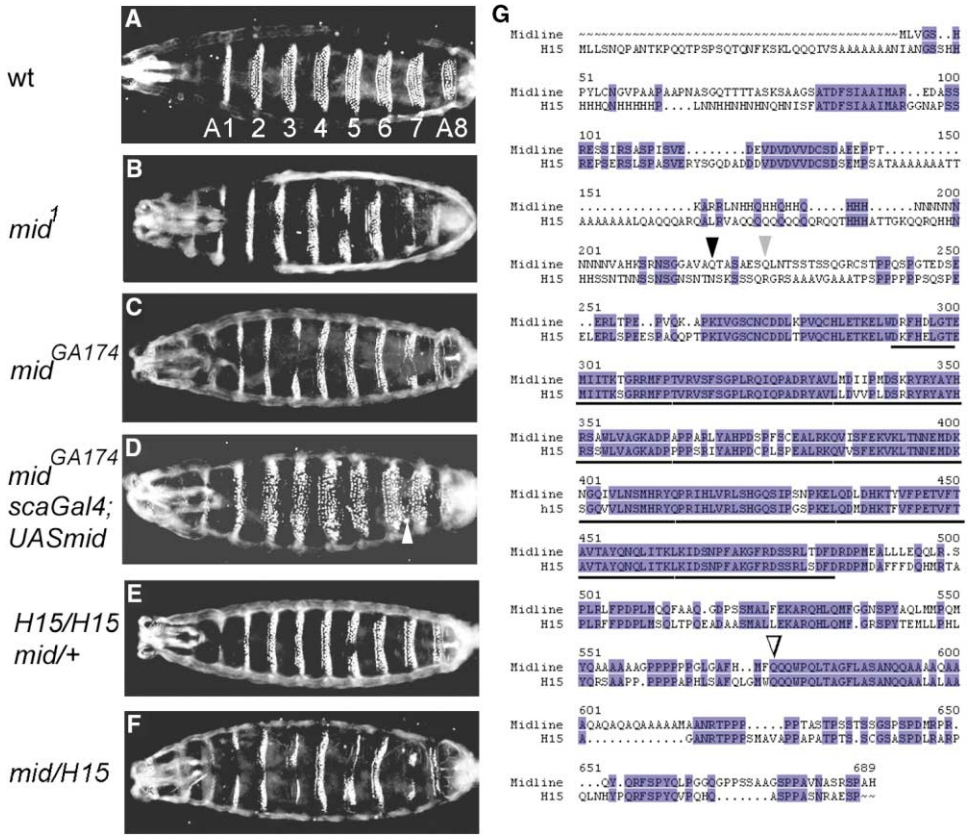

Figure 1. Midline and H15, Two Highly Homologous T Box Proteins, Are Required for Cuticle Patterning

(A) A wild-type larva (segments A1–A8 are marked).

(B) *mid*^{1} homozygote; note that the loss of denticles occurs predominantly in the ventral-most region of odd-numbered segments.

(C) *mid*^{GA174} homozygote.

(D) Rescue of the *mid*^{GA174} phenotype via the *sca*Gal4 driver in combination with UAS-*mid* (UAS-*CG6634*). Note that some ectopic denticles are formed between A6 and A7.

(E) *H15*^{x4}*/Df GpdhA*: this combination removes both copies of *H15* and one copy of *mid*.

(F) Overlapping deficiencies, *Df GpdhA* and *Df x528*, delete both copies of *mid* and *H15* (here referred to as *mid/H15*) and one uncharacterized gene, *CG31647*. Note that denticle rows 1–5, but not row 6, are missing in odd-numbered segments. (G) Protein sequence comparison of Mid and H15. Blue boxes indicate identical amino acids; the T box domain is underlined. The positions of the nonsense mutations are marked by triangles; a black triangle corresponds to *mid*^{1}, a gray triangle corresponds to *mid*^{GA174}, and an open triangle corresponds to *mid*^{2}.

Results and Discussion

Mutant alleles of *mid* (*mid*^{1}, *mid*^{2}), recessive embryonic-lethal zygotic mutations, were first identified in the classic screen for segmentation genes [14]. We isolated an additional allele, *mid*^{GA174}, from a collection of EMS-induced mutations [15]. *mid* mutant larvae are characterized by patches of naked cuticle in the ventral-most part of the abdominal denticle belts (Figures 1B and 1C). In addition, we occasionally observed a near-complete loss of denticle belts (or segmental halves of denticle belts). Both aspects of the phenotype are more pronounced in odd-numbered segment, whereas even-numbered segments show similar but milder defects. Genetic mapping has placed *mid* at cytological position 25E [14].

We examined this region for genes with expression patterns that suggest a role in segmentation. A P element insertion upstream of *H15 (CG6604)* displays a β-gal expression pattern consistent with such a role [16]. Both *H15* and an adjacent gene, *CG6634*, encode highly homologous T box proteins (Figure 1G) with essentially identical expression patterns (see below); thus, both genes represented candidates for *mid*. Deletion of *H15* by X-ray resulted in a homozygous pharate adult lethal line (*H15*^{x4}) with no appreciable cuticle phenotype. In contrast, sequencing of *CG6634* DNA from homozygous *mid*^{1}, *mid*^{2}, and *mid*^{GA174} embryos revealed nonsense mutations (Figure 1G). The putative translation products of *mid*^{1} and *mid*^{GA174} lack the DNA binding domain and are most probably nonfunctional. These data indicate that *CG6634* encodes the *mid* gene. This conclusion is corroborated by the observation that ectopic expression of *CG6634* in the *mid*^{1} mutant background rescues the cuticle defect (Figure 1D). To determine if, in the absence of Mid function, H15 contributes to cuticle formation, we examined early larvae lacking both copies of *H15* and one copy of *mid* (*H15*^{x4}*/Df-GpdhA*). We observed a weak *mid* phenotype (Figure 1E). Removal of both copies of *H15* and *mid* (hereafter referred to as *mid/*

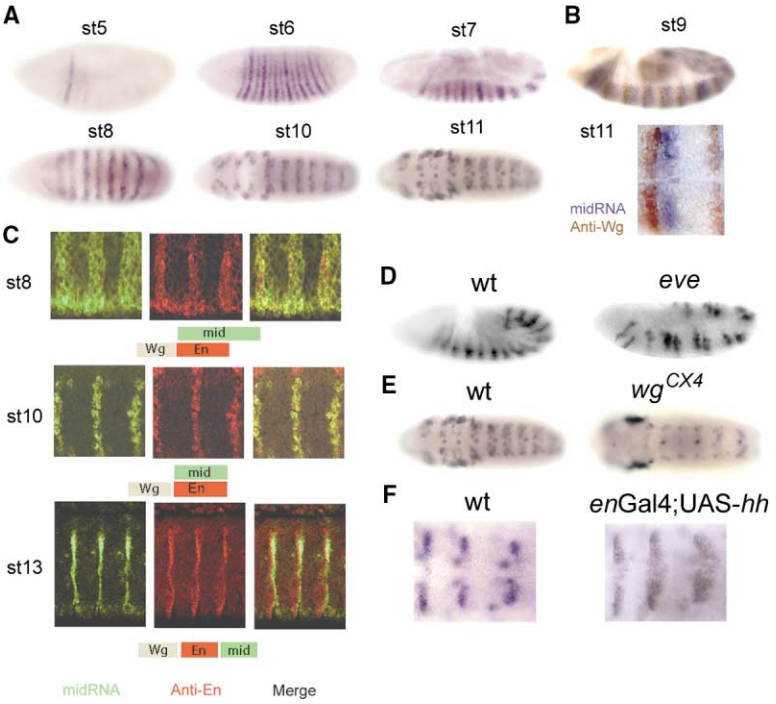

Figure 2. Expression Pattern and Regulation of *mid*

(A) From stage 5 to stage 11, *mid* is expressed in 14 ectodermal stripes, which (B) abut the posterior side of the Wg stripe. (C) The *mid*-expressing stripe undergoes dynamic changes and partially overlaps the En stripe (stage 8), colocalizes with En (stage 10), and abuts the posterior side of the En stripe (stage 13). (D) *mid* expression in stage 8 *eve* mutants. Note the altered spacing of the *mid* stripes. (E) In stage 11 *wg* mutants, *mid* expression decays prematurely (right panel). (F) Late *mid* expression (stage 13) is sensitive to Hh signaling; note the expanded *mid* stripes in the right panel. Anterior is to the left in all panels.

H15) resulted in a strong enhancement of the phenotype; the denticle rows 1–5 were frequently lost in odd-numbered segments, whereas even-numbered segments showed milder defects (Figure 1F). These findings suggest that Mid and H15 act redundantly to control denticle formation.

The *mid* RNA expression pattern is typical of segment polarity genes (Figure 2A). *H15* RNA expression pattern is identical with the exception that expression levels up to stage 9 are significantly lower than *mid* expression levels (data not shown). Fourteen stripes of *mid* expression are first detected in stage 5 embryos. Alternating stripes differ in width and intensity; even-numbered stripes are wider and show higher levels of expression. (Note that the first five *mid* stripes localize to the presumptive head and thoracic segments. Therefore, the even-numbered stripes 6, 8, 10, and 12 correspond to the stripes that are found in the odd-numbered abdominal segments 1, 3, 5, and 7.) During germband extension, expression becomes more uniform in consecutive stripes and is approximately equal in all stripes from stage 8 onward. *mid*-expressing stripes are maintained until the end of embryogenesis. However, *mid* expression occurs in distinct phases, during which it is regulated by different factors. Dynamic changes of the *mid* stripes with respect to width and location reflect the different regulatory inputs.

We first determined the precise location of the *mid* stripes by double labeling wild-type embryos with a *mid* RNA in situ probe and an anti-Wg antibody. During stages 5–11, *mid* expression abuts the posterior side of the Wg stripe (Figure 2B), but from late stage11 onward, the *mid* and the Wg stripes are separated by two rows of cells that express neither gene. The Wg and *mid* stripes remain separated until the end of embryogenesis. To determine the posterior limits of *mid* expression, we stained wild-type embryos with the *mid* RNA in situ probe and an anti-En antibody. Up to stage 9, *mid* expression is found in the En/Hh cells, but even-numbered *mid* stripes extend farther to include two rows of cells just posterior to the En/Hh domain. Weaker *mid* expression is found posterior to the En/Hh domain in odd-numbered segments (Figure 2C). This early expression of *mid* depends on pair-rule gene activity (for example, see Figure 2D; data not shown). By stage 10, the *mid*-expressing domain contracts to coincide with the En/Hh stripe. This stripe persists until early stage 11, after which *mid* expression in the En domain decays (Figure 2C). The maintenance of *mid* expression during stages 9–11 within the En domain requires Wg function; in *wg* null mutant embryos (wg^{CX4}), *mid* expression decays prematurely from stage 9 onward and is absent at stage 11 (Figure 2E). This dependence on Wg may provide a rationale for the narrowing of the *mid* stripe after initiation by the pair-rule genes because Wg signaling is not effective posterior to the En domain [17]. During late stage 11, *mid* expression is reinitiated in a 2- to 3-cell-wide stripe posterior to the En stripe. This stripe persists until the end of embryogenesis (Figure 2C). This late expression of *mid* is sensitive to Hh signaling; raising the level of Hh signaling (*en*Gal4; UAS-*hh*) results in a posterior expansion of the *mid* stripe (Figure 2F). It is noteworthy that this late expression of *mid* represents another example of an asymmetric outcome of bidirectional Hh signaling.

In odd-numbered abdominal segments, and to a lesser extent in even-numbered segments, concomitant loss of both Mid and H15 results in an excess of naked cuticle similar to that caused by ectopic Wg expression. To investigate if loss of Mid/H15 affects the Wg expression pattern, we stained double-mutant embryos with a anti-Wg antibody (Figures 3B and 3B′) or a *wg* RNA in

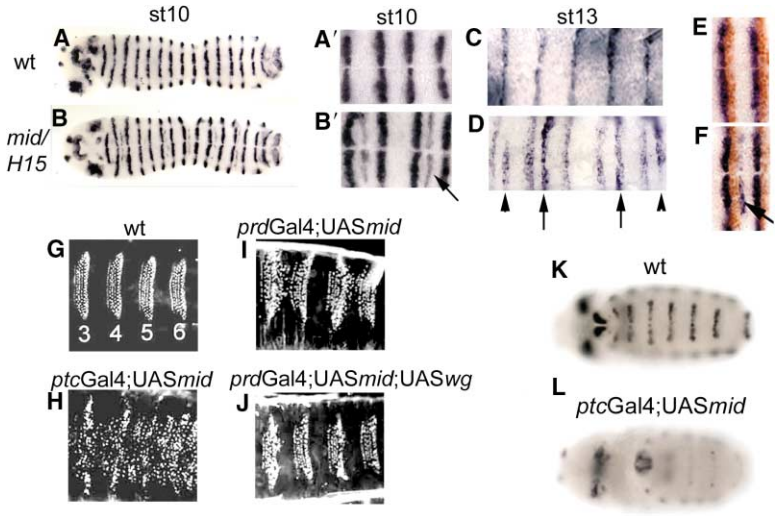

Figure 3. Loss of *mid/H15* Results in a Hh-Dependent Ectopic Expression of Wg, and Misexpression of *mid* Represses *wg*

(A) Wild-type and (B) *mid/H15*: Wg protein distribution in stage 10 embryos; note that extra stripes of Wg appear in alternating segments. (A′) Wild-type and (B′) *mid/H15*: high-magnification views of Wg protein distribution at stage 10. (C) Wild-type and (D) *mid/H15*: Wg protein in stage 13 embryos. Arrows indicate ectopic Wg in odd-numbered segments; arrowheads indicate ectopic Wg in even-numbered segments. (E) In the wild-type, the Wg stripe abuts the En stripe at the anterior end. (F) In *mid/H15* homozygotes, the En stripe is symmetrically straddled by Wg stripes. Misexpression of *mid* mimics a late loss of *wg* phenotype. (G) Wild-type and (H) (*ptc*Gal4;UAS-*mid*), cuticle phenotype of first-instar larvae. (I) *prd*Gal4;UAS-*mid* and (J) (*prd*Gal4;UAS-*mid;* UAS-*wg*), cuticle pheno type of first-instar larvae. Note the near-complete lack of denticle belt fusions in (J) compared to (I). (K) Wild-type and (L) (*ptc*Gal4;UAS-*mid*) Anti-Wg staining of stage 11 embryos. Note the almost complete loss of Wg. Anterior is to the left in all panels except (K) and (L), which show anterior to the right.

situ probe (data not shown). From stage 9 onward, we observed ectopic 1-cell-wide Wg stripes in odd-numbered abdominal segments and occasionally found weak patches of ectopic Wg in even-numbered segments. The initially weak ectopic stripes subsequently increased in intensity so that by stage 13 high levels of ectopic Wg were found in odd-numbered segments and lower levels of ectopic Wg were seen in some even-numbered segments (Figure 2D). Hence, the pair-rule-biased pattern of ectopic Wg expression reflects the defect observed in *mid/H15* larval cuticles; namely, this defect is a gain of naked cuticle predominantly, but not exclusively, in odd-numbered segments. Ectopic Wg expression was also found in stage 9 *mid* single mutants, albeit less frequently and less robustly. It was also observed very rarely in *H15* single mutants (data not shown). We determined the precise location of the ectopic Wg expression by double staining *mid/H15* mutant embryos with anti-Wg and anti-En antibodies. The ectopic Wg stripes abut the posterior side of the En stripes (within the domain of early *mid* expression; see Figure 7G for the localization of the early *mid* expression domain), generating a pattern in which En-expressing cells are straddled by Wg-expressing cells (Figure 3F).

To assess the effects of *mid* gain-of-function on Wg expression, we used several Gal4 drivers to misexpress *mid*. We first examined the cuticle phenotype of the resulting larvae; this phenotype represents a highly sensitive read-out of even small changes in the level of Wg signaling. The cuticle phenotype of *ptc*Gal4;UAS-*mid* (Figures 3G and 3H) and *sca*Gal4;UAS-*mid* (data not shown) larvae mimicked that of a late loss of *wg* function; in the posterior half of the larvae, nearly all naked cuticle was replaced with denticles. In the anterior half, extra denticles appeared predominantly in the ventral-most region. This phenotype appeared with 100% penetrance. In addition, *ptc*Gal4;UAS-*mid* larvae (and to a lesser extent *sca*Gal4;UAS-*mid* embryos) showed specific morphological defects characteristic of *wg* loss-of-function mutants: reduced body size, strong segmental indentations, and malformation of the head. To confirm that the cuticle defects caused by ectopic Mid were due to decreased Wg expression, we expressed UAS-*mid*, UAS-*wg*, or both under the control of *prd*Gal4, which is strongly expressed in the Wg domain in the even-numbered abdominal segments. Coexpression of *wg* with *mid* resulted in near-complete suppression of the fusion of alternating denticle belts as a result of misexpression of *mid* alone (Figures 3I and 3J). The cuticle defects observed in *ptc*Gal4;UAS-*mid* larvae were matched by altered levels of Wg protein (Figures 3K and 3L); from stage 10 onward, Wg protein in the ventral ectoderm decayed, and at stage 13 it was nearly absent in the ventral epidermis. Hence, misexpression of *mid* is sufficient to antagonize Wg in its endogenous expression domain.

The appearance of the ectopic Wg stripes in *mid/H15* mutants coincides with the stabilization phase of the endogenous Wg expression by Hh signaling. The endogenous Wg expression (anterior to the En/Hh stripe) was not affected in either *mid* single or *mid/H15* double mutants at any time, suggesting that Hh signaling is normal. To corroborate this conclusion, we examined the expression of the *hh* gene, the distribution of Hh protein, and the effect of Hh signaling on the expression of the *ptc* gene. *ptc*RNA expression in narrow stripes anterior and posterior to the En domain has been shown to be a read-out of bidirectional Hh signaling [10, 11]. We observed no difference in the *hh* and *ptc* expression patterns in wild-type and *mid/H15* embryos (Figures 4A and 4B and data not shown). This demonstrates that the regulatory interactions that result in the maintenance of endogenous Wg at stage 9 and the autoregulation of Wg from stage 11 onward function normally in *mid/H15* double mutants. This raises the possibility that Hh signaling may activate Wg expression in a symmetrical manner but that expression of Wg posterior to the En stripe is antagonized by Mid/H15. To investigate this possibility, we studied the effects of manipulating Hh signaling in a *mid/H15* mutant background. First, when

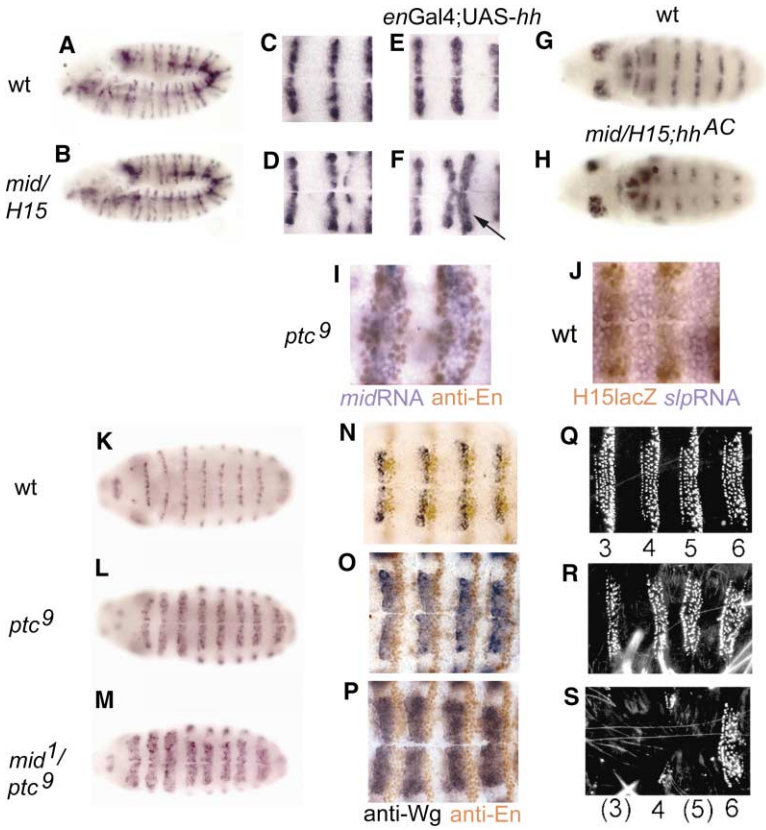

Figure 4. The Levels of Hh Signaling Control the Spatial Limits of Ectopic *wg* Expression

(A) Wild-type and (B) *mid/H15*. *ptc* RNA in situ: Note that *ptc* RNA distribution in stage 11 embryos is normal. (C) Wild-type, (D) *mid/H15*, (E) *en*Gal4;UAS-*hh*, and (F) *Df GpdhA/en*Gal4, *Df x528;*UAS-*hh*: Note the posterior expansion of the ectopic Wg stripe. In (F) the arrow indicates the ectopic Wg stripe. (G) Wild-type and (H) (*Df GpdhA/Df x528*; hh^{AC}) Wg expression at stage 11. Note the absense of ectopic Wg in the *hh* mutant background and the decay of endogenous Wg. (I) *mid* RNA and En protein distribution in *ptc* mutant embryos: Note that *mid* RNA fills the entire space between the endogenous and ectopic En stripes. (J) Distribution of H15 (anti-β-gal staining) and *slp* RNA: Note that both expression domains are nonoverlapping and separated by one row of cells expressing *slp*, *mid*, or neither. (K–M) *wg* RNA distribution in (K) wild-type, (L) ptc^9, and (M) mid^1ptc^9 stage 11 embryos. In ptc^9 embryos the *wg* stripe is expanded, and in mid^1ptc^9 embryos it is expanded even further. In (M) note that consecutive *wg* stripes form pairs. (N–P) Wg protein and En protein distribution in stage 11 embryos. (N) Wild-type and (O) ptc^9: Note the ectopic En stripe in all segments. (P) mid^1ptc^9: Note that in alternating segments all cells express either *wg* or *en*. (Q–S) cuticle pattern of (Q) wild-type, (R) ptc^9, or (S) mid^1ptc^9 larvae. In (S) note that odd-numbered denticle belts are completely lost. Anterior is to the left in all panels except (G) and (H).

we raised the level of Hh signaling from within the endogenous Hh/En domain (*en*Gal4;UAS-*hh*), the ectopic Wg expanded to a 2- to 3-cell-wide stripe, thus demonstrating that the level of Hh controls the spatial limits of ectopic Wg expression (Figure 4F). Reciprocally, in *hh/mid/H15* triple mutants, no ectopic Wg expression was observed (Figure 4H). These data show that Hh signals symmetrically with respect to cells anterior and posterior to the En/Hh stripe; Mid and H15 are required to prevent posterior Wg expression, thus ensuring that Wg expression remains restricted to a single domain.

Loss of *mid/H15* leads to ectopic Wg expression in a single row of cells. As shown above, raising the level of Hh signaling (*mid/H15;en*Gal4;UAS-*hh*) results in an expansion of the ectopic Wg stripe. To unmask the potential of cells to express Wg in the absense of Mid-mediated repression, we examined mid^1ptc^9 double-mutant embryos in which Wg expression is largely independent of Hh. In *ptc* mutant embryos, the expression domain of Wg broadens in the anterior direction, and ectopic En expression is induced de novo in cells anterior to these broadened domains [12]. The anterior region of the segment between the ectopic En stripe and the next endogenous En stripe does not express Wg (Figure 4O). Double labeling of *ptc* embryos with the *mid* RNA in situ probe and anti-En antibody showed that *mid* fills this region (Figure 4I). Removal of Mid function caused all cells in odd-numbered segments to express either Wg or En (but not both) (Figure 4P) and resulted in a complete loss of the odd-numbered denticle belts (Figure 4S).

Close examination revealed some unexpected features: the *wg* transcription domain is slightly widened in mid^1ptc^9 embryos as compared to *ptc* single mutants; however, this occurs in all segments without any pair-rule bias. Moreover, consecutive *wg RNA* stripes form pairs (1-2, 3-4, and so on) that are separated by wider gaps from the subsequent pair (Figure 4M). The region between two partners of each *wg* pair is entirely filled with En-expressing cells, suggesting a fusion of the ectopic and the endogenous En domains (Figure 4P). Taken together, these data indicate that concomitant loss of *mid* and *ptc* results in defects that go beyond a simple change of Wg and En expression. This notion is supported by the observation that, as compared to even-numbered segments, odd-numbered segments in mid^1ptc^9 embryos are shorter by approximately two rows of cells (data not shown). Future studies will show if *mid* plays a role in proper segment formation, which requires cell survival, cell division, and cell sorting.

Earlier studies of the regulation of Wg expression showed that loss of *ptc* results in an anterior expansion of the *wg* transcription domain. It does not, however, result in ectopic Wg expression posterior to the En domain. To rationalize this asymmetric response of the *wg* promoter to bi-directional Hh signaling, it was proposed that each parasegment is divided into two domains: the posterior half of the parasegment represents the *wg*-competent domain and the anterior half is the *en*-compentent domain [12]. Wg-competence requires the *slp* genes which are expressed in broad stripes anterior to the En/Hh stripe (see Figure7G for the localization of

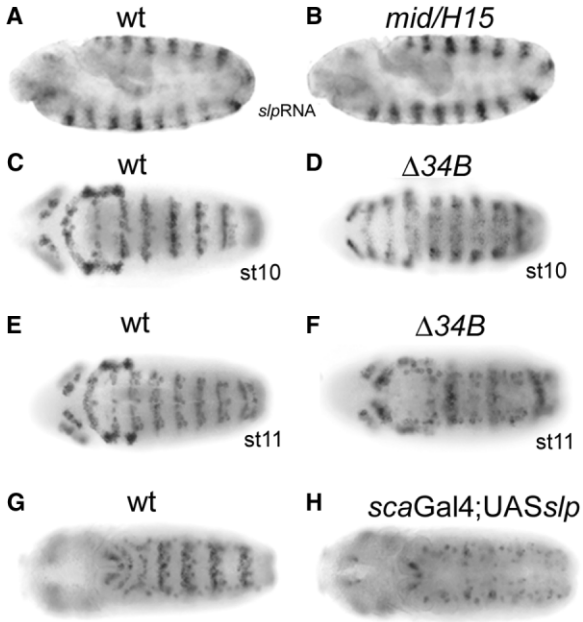

Figure 5. Regulatory Interactions of *slp* and *mid*. (A) Wild-type and (B) *mid/H15*: *slp* RNA distribution. (C–H) *mid* RNA distribution in wild-type (C and E) or *slpΔ34B* mutant (D and F) embryos. Note the expansion of the *mid* stripes in (D) and the subsequent decay of *mid* in (F). (G) Wild-type and (H) *sca*Gal4;UAS-*slp1* embryos. Note that misexpression of *slp* results in the loss of epidermal *mid* expression. The remaining *mid* staining labels neuroblasts and their progenies. Anterior is to the left in all panels except (G) and (H).

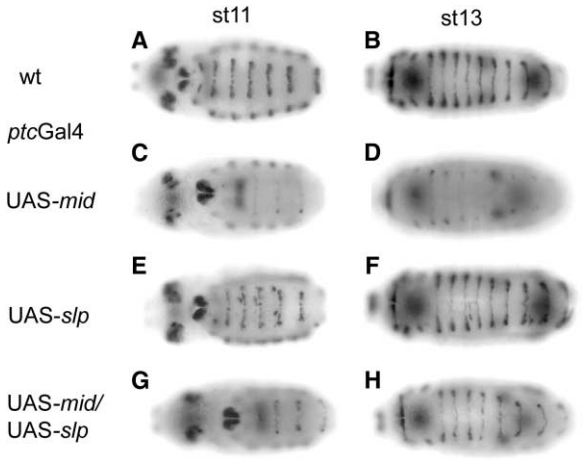

Figure 6. Misexpression of *mid* and/or *slp* Results in Aberrant Wg Expression Patterns

(A–H): Anti-Wg antibody staining. (A and B) wild-type. (C–H) Misexpression via the *ptc*Gal4 driver. (C and D) UAS-*mid*: Note the almost complete loss of Wg. (E and F) UAS-*slp*: Note some ectopic expression of Wg. (G and H) UAS-*mid*/UAS-*slp*: Note that there is no ectopic Wg. Note also a reduction of endogenous Wg expression.

the *slp*-expressing domain) [13]. We have shown here that loss of *mid/H15* results in the ectopic expression of Wg within the *en*-competent domain (where Slp is absent). This prompted us to study any possible regulatory interactions between *slp* and *mid/H15*. Double staining of *H15-lacZ* embryos (which are viable and wild-type with respect to Wg expression) with a *slp* in situ probe and anti-β-*gal* antibody showed that, at stage 9, *slp* and *H15 (mid)* are expressed in non-overlapping domains that are separated by one row of cells in the center of each segment. Within this central row, *slp*-positive and *mid*-positive cells intermingle with cells expressing neither gene (Figure 4J).

It is conceivable that the ectopic expression of Wg in *mid/H15* mutant embryos could be a secondary effect brought about by a gain of Slp expression posterior to the En stripe. RNA in situ analysis revealed no change of the Slp expression pattern in *mid/H15* embryos (Figures 5A and 5B). Hence, in odd-numbered segments of wild-type embryos, the lack of *wg* competence in the cells immediately posterior to the En/Hh stripe is a consequence of Wg repression via Mid/H15 rather than of a lack of activation via Slp.

Previous work has suggested that Slp permits the Hh-dependent activation of Wg anterior to the En/Hh stripe by antagonizing a repressor of Wg. Based on the data presented above, Mid/H15 appear to be such repressors. To determine if Slp is a negative regulator of *mid* expression, we examined the effect of *slp* loss-of-function and *slp* misexpression on the distribution of *mid* RNA. In *slp* mutant embryos (*Δ34B),* the early *mid* expression is normal. However from early stage 9 onward the *mid* stripes broaden to approximately twice their normal width (Figure 5D). Using *mid*-positive neuroblasts as a landmark (these remain unchanged in *slp* mutant embryos), we were able to characterize the increase in *mid* expression as an anterior expansion. This aberrant *mid* expression pattern is unstable; from stage 11 onward *mid* decays in odd-numbered segments (Figure 5F). Conversely, misexpression of *slp* in the ventral ectoderm from early stage 9 onward led to a complete loss of ectodermal *mid* expression (Figure 5H). These data show that Slp functions as a repressor of *mid* expression. Taken together with the observation that misexpression of *mid* in otherwise wild-type embryos results in the loss of Wg expression, these results lead us to conclude that the Slp-mediated repression of *mid* anterior to the En/Hh stripe is an important component of *wg* competence.

As a further test of the relationship between *slp* and *mid*, we compared the effect of expressing *mid* and *slp*, alone or in combination, on Wg expression. Ectopic expression of *mid* results in a rapid and almost complete loss of Wg expression, whereas ectopic expression of *slp* results in weak ectopic expression of Wg posterior to the En/Hh stripe (Figures 6A–6F). This *slp*-induced phenotype resembles that of the loss of *mid*, except that ectopic Wg expression is weaker and appears randomly in even- and odd-numbered segments (Figures 6E and 6F). The ectopic Wg expression is blocked when *mid* and *slp* are expressed together, suggesting that in this context *mid* acts downstream of *slp*. The Wg expression anterior to the En/Hh stripe still decays in UAS-*mid*/UAS-*slp* embryos, albeit more slowly and variably than in UAS-*mid* alone. This result may reflect that Wg expression is sensitive to the amounts of available Mid and Slp. It may also indicate that anterior to the En/Hh stripe, Slp function is required for more than just

repression of *mid* and may possibly have independent activating functions. An analysis of *slp1,slp2;mid/H15* quadruple mutants would be highly helpful in clarifying the relationship between *slp* genes and *mid/H15*. Unfortunately, the generation of such a quadruple mutant by genetic recombination is impossible because the *slp* deletion that removes these genes (Δ34B) is on a balancer chromosome that precludes recombination.

The pair-rule modulation of the *mid/H15* deletion phenotype results from a different requirement in alternate segments for *mid/H15*-mediated repression of Wg downstream of Hh signaling. However, in *mid/H15* mutant larvae, even-numbered denticle belts also show some defects. This prompted us to determine if *mid/H15* plays a role in the expression of other regulators of late segmental patterning. After stage 11, Wg and Hh signaling regulate other target genes, resulting in the subdivision of each segment into smaller territories. In the posterior, adjacent to the En/Hh-expressing cells, a Rhomboid (Rho)-expressing domain is created [18, 19]. Rho processes membrane bound, inactive Spitz (Spi) to an active, secreted form [18]. Competing Spi and Wg signaling control the decision between naked cuticle and denticle formation, with Spi activating denticle-type specification and Wg specifying naked cuticle [20, 21]. After stage 11, the *mid* stripe marks the anterior most rows of cells in every segment and colocalizes with *rho*. In situ hybridization of stage 13 *mid/H15* mutants with a *rho*-specific probe revealed a reduction/absence of *rho* expression in odd-numbered abdominal segments (Figures 7A and 7B), suggesting that the excess of naked cuticle in *mid/H15* mutant larvae arises from the gain of Wg and the concomitant loss of Spi signaling. We also examined the expression of Serrate (Ser), which is normally restricted to cells posterior of Rho in abdominal segments because of repression by Hh signaling (see Figure 7G for the expression domain of Ser) [22]. The Ser domain expands into the Rho domain at the anterior end of the segment in embryos lacking *mid* (Figures 7C and 7D), whereas Ser expression is lost completely in embryos with ectopic *mid* expression (Figures 7E and 7F). This suggests that Mid acts downstream of Hh signaling to repress Ser in addition to Wg. The anterior expansion of Ser in every segment may contribute to the defects found in even-numbered segments, in which only variable weak ectopic Wg expression is detected.

The data we have presented here indicate that *mid/H15* are negative regulators of Wg and Ser. In the ventral ectoderm of odd-numbered abdominal segments, *mid/H15* act to break the symmetry of the Hh-dependent activation of Wg expression (see model in Figure 7G). In 1991, Ingham and coworkers proposed that pair-rule gene activity leaves "imprints" on all cells and that these imprints predispose cells to express either Wg or En [12]. Later, Slp was found to be such an "imprint" anterior to the En/Hh stripe, where it predisposes cells to express Wg [13]. The early, pair-rule gene-driven *mid/H15* expression appears to be another such "imprint" that predisposes cells posterior to the En/Hh stripe not to express Wg.

Our findings raise several questions. First, because the outcome of bidirectional Hh signaling is asymmetric in all abdominal segments, additional factors that prevent the inappropriate expression of Wg in even-numbered segments must exist. At present, such factors are not known. Also, is the decreased Rho expression in alternating segments a direct consequence of a loss of activation by *mid/H15* or a result of negatively acting, ectopic Wg expression? We favor the latter explanation because the ectopic pair-rule-biased expression of Wg corelates with the pair-rule-biased loss of Rho, and ectopic activation of the Wg pathway is sufficient to repress Rho expression posterior to the En/Hh stripe. Finally, what is the molecular mechanism of Wg repression by *mid/H15*? Mid and H15 are members of the T box family of transcription factors and therefore presumably modulate target gene expression directly. The target genes of Mid/H15 are currently unknown. Although it is conceivable that *wg* is a direct target gene, other scenarios are possible: Mid/H15 may positively or nega-

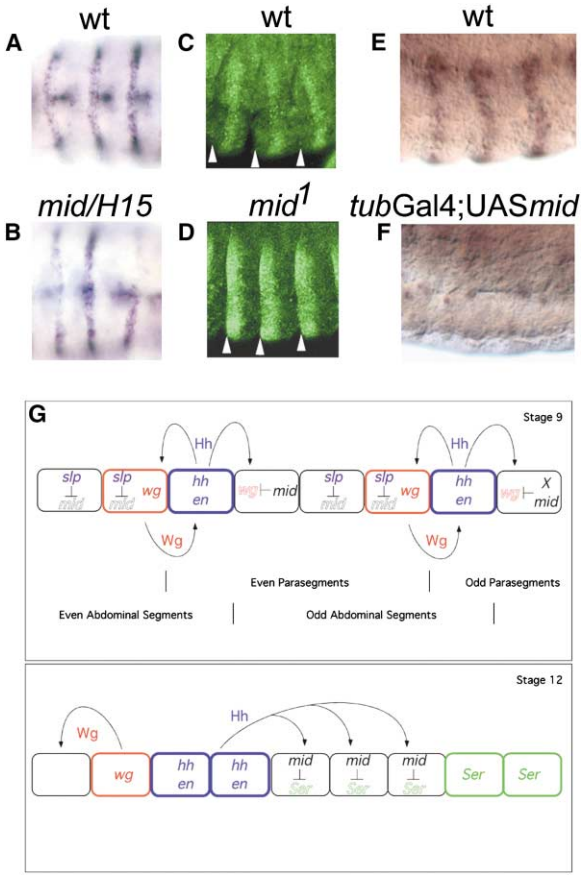

Figure 7. *rho* and *ser* Expression in Wild-Type and Mutant Embryos

(A) Wild-type and (B) *mid/H15*. *rho* is reduced/absent in odd-numbered segments in *mid/H15* embryos. (C) Wild-type and (D) *mid*^{1}: Ser protein in stage 13 embryos. The Ser domain expands anterior to the segment border in *mid*^{1} (white arrowheads). (E) Wild-type and (F) *Tub*Gal4;UAS-*mid*: *ser* RNA expression is lost when *mid* is expressed ectopically. Anterior is to the left. (G) A model for *mid/H15* function in segmentation. In stage 9 embryos, *mid* (and *H15*) prevents the activation of *wg* by Hh in cells posterior to the *en* domain. An unknown factor ("X") is required for *wg* repression in alternating segments. In stage 12 embryos, *mid* (and *H15*) is required for the repression of *ser* in the anterior of the each segment. We speculate that *mid* may be activated in this domain by both Hh and Ser signaling.

tively regulate the expression of unidentified genes and thereby modulate Wg or Hh pathway activities, and hyperactivity of either pathway could produce an ectopic stripe of Wg expression. It is noteworthy that a different group of T box genes, the *dorsocross* genes, has been identified as a negative regulator of Wg expression in the dorsolateral epidermis [23]. However, the Dorsocross target genes are also unknown. Further studies are required to elucidate the mechanisms by which T box proteins negatively regulate Wg expression.

Experimental Procedures

Fly Strains

The alleles *mid*^{1} and *mid*^{2} were obtained from the Bloomington stock center [14]. *mid*^{GA174} was isolated from a collection of EMS-induced mutations [15]. The deficiencies *H15*^{x4} and *Df(2L)x528* were generated by X-irradiation, and the breakpoints were determined by PCR analysis. *Df-GpdhA* (breakpoints 25D7; 26A2-5) was obtained from the Bloomington Stock Center, and the breakpoints were determined by PCR analysis. *ptc*^{9}, *wg*^{CX4}, *hh*^{AC} and *slp*$^{\Delta 34B}$ are null alleles (see Flybase: http://www.flybase.org). All mutant alleles were balanced over *CyO*^{ftzlacZ} or *CyO*^{wglacZ} to facilitate the identification of homozygotes. *en*Gal4 (a gift from A. Gould; originally generated by A. Brand), *sca*Gal4 (a gift from X. Yang; *sca*Gal4 drives expression in the ventral ectoderm from early stage 9 onward), *ptc*Gal4, *Tub*-Gal4, and *prd*Gal4 (Bloomington Stock Center) were used to drive the expression of transgenes. UAS-*hh.1* and UAS-*slp1* (on the third chromosome) were a gift from M. Frasch; UAS-slp1 (on the second chromosome) was a gift from M. Leptin. UAS-*wg* was a gift from A. Simmonds. A transgenic stock carrying UAS-*CG6634* (UAS-*mid.1.4*; insertion on the third chromosome) was generated from the full-length *CG6634* cDNA (derived from RE27439) subcloned into the pUAST vector.

All strains were raised at 22°C on standard corn meal agar medium.

Cloning of *mid*

mid^{1}, *mid*^{2}, and *mid*^{GA174} were balanced over CyO^{ActGFP} to facilitate the identification of homozygous mutant embryos. Genomic DNA was isolated according to standard protocols and analyzed by automated sequencing. *mid*^{1} was found to have a C-to-T transition at position 659, *mid*^{2} to have a C-to-T transition at position 1758, and *mid*^{GA174} to have a C-to-T transition at position 680; numbering is according to the cDNA clone RE27439. All three base pair substitutions result in nonsense codons.

Phenotypic Analysis

Immunohistochemistry. Embryos were collected, fixed, and immunostained as previously described [24]. Primary antibodies were polyclonal rat anti-Serrate (a gift from K. Irvine) and monoclonal mouse anti-Engrailed/Invected (4D9) and mouse anti-Wingless (4D4). The respective hybridomas, developed by C. Goodman (4D9) and S.M. Cohen (4D4), were obtained from the Developmental Studies Hybridoma Bank developed under the auspices of the National Institute of Child Health and Human Development (NICHD) and maintained by The University of Iowa, Department of Biological Sciences, Iowa City, IA 52242. Histochemical detection was performed with Jackson Immunoresearch HRP-conjugated secondary antibodies and visualized by the glucose-oxidase-DAB-nickel method as previously described [24].

RNA in situ hybridization was carried out as described previously [25]. Fluorescent RNA in situ hybridization was performed with the TSA Fluorescein System from PerkinElmer according to the manufacturer's instruction. For generation of a *mid*-specific RNA in situ probe, 1.1 kb of 5′ cDNA sequence (derived from RE27439) was subcloned into Bluescript vector and subsequently transcribed in vitro with T7 RNA polymerase. A construct for the generation of a *rho*-specific RNA probe was a gift from A. Gould. A *slp*-specific RNA in situ probe was generated by in vitro transcription of full-length *slp* cDNA with SP6 polymerase.

Cuticles of first-instar larvae were prepared essentially as described [7] except that the vitelline membranes were removed by vigorous agitation in methanol/heptane (1:1). The larvae were then placed in a microtube and incubated overnight at 55°C in a mixture of Hoyer's medium/lactic acid (1:1). Subsequently, the larvae were mounted on slides and viewed with dark-field microscopy.

Acknowledgments

We thank A. Gould, M. Frasch, A. Simmonds, K. Irvine, X.H. Yang, and the Bloomington Stock Center for providing materials; P.W. Ingham, S. DiNardo, and P. Overton for helpful comments on the manuscript; and P. Overton for help in preparing Figure 1. W.J.B. is supported by the Canadian Institutes of Health Research and the Alberta Heritage Foundation for Medical Research.

Received: March 12, 2004
Revised: August 6, 2004
Accepted: August 6, 2004
Published: October 5, 2004

References

1. St Johnston, D., and Nusslein-Volhard, C. (1992). The origin of pattern and polarity in the Drosophila embryo. Cell *68*, 201–219.
2. Lee, J.J., von Kessler, D.P., Parks, S., and Beachy, P.A. (1992). Secretion and localized transcription suggest a role in positional signaling for products of the segmentation gene hedgehog. Cell *71*, 33–50.
3. Mohler, J., and Vani, K. (1992). Molecular organization and embryonic expression of the hedgehog gene involved in cell-cell communication in segmental patterning of Drosophila. Development *115*, 957–971.
4. Bejsovec, A., and Martinez Arias, A. (1991). Roles of wingless in patterning the larval epidermis of Drosophila. Development *113*, 471–485.
5. Martizenz Arias, A., Baker, N.E., and Ingham, P.W. (1988). Role of segment polarity genes in the definition and maintenance of cell states in the Drosophila embryo. Development *103*, 157–170.
6. Baker, N.E. (1988). Localization of transcripts from the wingless gene in whole Drosophila embryos. Development *103*, 289–298.
7. DiNardo, S., Heemskerk, J., Dougan, S., and O'Farrell, P.H. (1994). The making of a maggot: patterning the Drosophila embryonic epidermis. Curr. Opin. Genet. Dev. *4*, 529–534.
8. Hatini, V., and DiNardo, S. (2001). Divide and conquer: pattern formation in Drosophila embryonic epidermis. Trends Genet. *17*, 574–579.
9. Sanson, B. (2001). Generating patterns from fields of cells. Examples from Drosophila segmentation. EMBO Rep. *2*, 1083–1088.
10. Hidalgo, A., and Ingham, P. (1990). Cell patterning in the Drosophila segment: spatial regulation of the segment polarity gene patched. Development *110*, 291–301.
11. Forbes, A.J., Nakano, Y., Taylor, A.M., and Ingham, P.W. (1993). Genetic analysis of hedgehog signalling in the Drosophila embryo. Dev. Suppl., 115–124.
12. Ingham, P.W., Taylor, A.M., and Nakano, Y. (1991). Role of the Drosophila patched gene in positional signalling. Nature *353*, 184–187.
13. Cadigan, K.M., Grossniklaus, U., and Gehring, W.J. (1994). Localized expression of sloppy paired protein maintains the polarity of Drosophila parasegments. Genes Dev. *8*, 899–913.
14. Nusslein-Volhard, C., Wieschaus, E., and Kluding, H. (1984). Mutations affecting the pattern of the larval cuticle in Drosophila melanogaster. I. Zygotic loci on the second chromosome. Roux Arch. Dev. Biol. *193*, 267–282.
15. Seeger, M., Tear, G., Ferres-Marco, D., and Goodman, C.S. (1993). Mutations affecting growth cone guidance in Drosophila: genes necessary for guidance toward or away from the midline. Neuron *10*, 409–426.
16. Griffin, K.J., Stoller, J., Gibson, M., Chen, S., Yelon, D., Stainier, D.Y., and Kimelman, D. (2000). A conserved role for H15-related

T-box transcription factors in zebrafish and Drosophila heart formation. Dev. Biol. *218*, 235–247.

17. Sanson, B., Alexandre, C., Fascetti, N., and Vincent, J.P. (1999). Engrailed and Hedgehog make the range of Wingless asymmetric in *Drosophila* embryos. Cell *98*, 207–216.
18. Schweitzer, R., Shaharabany, M., Seger, R., and Shilo, B.Z. (1995). Secreted Spitz triggers the DER signaling pathway and is a limiting component in embryonic ventral ectoderm determination. Genes Dev. *9*, 1518–1529.
19. Alexandre, C., Lecourtois, M., and Vincent, J. (1999). Wingless and Hedgehog pattern Drosophila denticle belts by regulating the production of short-range signals. Development *126*, 5689–5698.
20. Szuts, D., Freeman, M., and Bienz, M. (1997). Antagonism between EGFR and Wingless signalling in the larval cuticle of Drosophila. Development *124*, 3209–3219.
21. Payre, F., Vincent, A., and Carreno, S. (1999). ovo/svb integrates Wingless and DER pathways to control epidermis differentiation. Nature *400*, 271–275.
22. Wiellette, E.L., and McGinnis, W. (1999). Hox genes differentially regulate Serrate to generate segment-specific structures. Development *126*, 1985–1995.
23. Reim, I., Lee, H.H., and Frasch, M. (2003). The T-box-encoding Dorsocross genes function in amnioserosa development and the patterning of the dorsolateral germ band downstream of Dpp. Development *130*, 3187–3204.
24. Yang, X., Bahri, S., Klein, T., and Chia, W. (1997). Klumpfuss, a putative Drosophila zinc finger transcription factor, acts to differentiate between the identities of two secondary precursor cells within one neuroblast lineage. Genes Dev. *11*, 1396–1408.
25. Tautz, D., and Pfeifle, C. (1989). A non-radioactive in situ hybridization method for the localization of specific RNAs in Drosophila embryos reveals translational control of the segmentation gene hunchback. Chromosoma *98*, 81–85.